Synergistic regenerative therapy of thin endometrium by human placenta-derived mesenchymal stem cells encapsulated within hyaluronic acid hydrogels

Yifeng Lin
Zhejiang University
Shunni Dong
Zhejiang university
Xiaohang Ye
Zhejiang University
Juan Liu
Zhejiang University
Jiaqun Li
Zhejiang University
Yanye Zhang
Zhejiang University
Mixue Tu
Zhejiang University
Siwen Wang
Zhejiang University
Yanyun Ying
Zhejiang University
Ruixue Chen
Zhejiang University
Feixia Wang
Zhejiang University
Feida Ni
Zhejiang University
Jianpeng Chen
Zhejiang University
Binyang Du
Zhejiang University
Zhang Dan (zhangdan@zju.edu.cn)
Zhejiang University https://orcid.org/0000-0003-1295-4795

Research

Keywords: Human placenta-derived mesenchymal stem cells, Hyaluronic acid hydrogels, Thin endometrium, Endometrial repair, Regeneration mechanisms

Posted Date: July 26th, 2021

DOI: https://doi.org/10.21203/rs.3.rs-729870/v1

Version of Record: A version of this preprint was published at Stem Cell Research & Therapy on February 8th, 2022. See the published version at https://doi.org/10.1186/s13287-022-02717-2.

Abstract

Background: Endometrial injury is one of the major causes of thin endometrium and subfertility. Stem cell-based therapies have made strides towards further efficacious treatment of injured endometrium. However, reported therapeutic stem cells that can be used for thin endometrium are difficult to acquire for large-scale clinical application. The human placenta-derived mesenchymal stem cells (HP-MSCs) are emerging alternative sources of MSCs for their robuster expansion ability, lower immunogenicity as well as extensive sources. To maximize their retention inside the uterus, we loaded HP-MSCs with cross-linked hyaluronic acid hydrogel (HA hydrogel) to investigate their therapeutic efficacy and possible underlying mechanisms.

Methods: The murine endometrial injury model was established by ethanol (95%) perfusion, with further intrauterine instillation of treating materials. The retention time of HP-MSCs was detected by *in vivo* imaging and *ex vivo* frozen section. Functional restoration of the uterus was assessed by testing embryo implantation rates. The endometrial morphological alteration was observed by H&E staining, Masson staining, and immunohistochemistry (Ki67). The stromal and glandular cells were isolated from the human endometrium to determine proliferation, migration, signaling pathway changes via EdU assay, transwell migration assay, and western blot respectively.

Results: Instilled HP-MSCs with HA hydrogel (HP-MSCs-HA) exhibited a prolonged retention time in mouse uteri compared with normal HP-MSCs. *In vitro* data showed that the HP-MSCs-HA could significantly increase the gland number and endometrial thickness, decrease fibrous area, promote the proliferation of endometrial cells, and improve the embryo implantation rate. *In vitro* assays indicated that HP-MSCs-HA could not only promote the proliferation and migration of human endometrial stromal via the JNK/Erk1/2-Stat3-VEGF pathway but also promote the proliferation of glandular cells via Jak2-Stat5 and c-Fos-VEGF pathway.

Conclusion: Our study suggested the potential therapeutic effects and the underlying mechanisms of HP-MSCs-HA on treating thin endometrium. HA hydrogel could be a preferable delivery method for HP-MSCs and the strategy represents a promising therapeutic approach against endometrial injury in clinical settings.

Background

Embryo quality and intrauterine environment are key factors in physiological pregnancy for women of childbearing age. Despite the breakthrough in improving embryo quality by assisted reproductive technologies (ART), the implantation rate is still lower than expected, which implies the necessity and cruciality of a receptive endometrium with proper thickness [1]. However, physical (induced abortion, frequent intrauterine operation, radiation) and biochemical (infection, endocrine-disrupting chemical) injury will impair the normal growth of the endometrium, which can contribute to thin endometrium, a common disease in women of reproductive age [2, 3]. In assisted reproduction, an endometrial thickness

of 8–12 mm is considered to normal for embryo implantation, a thickness of less than 7–8 mm is commonly defined as thin endometrium [3–6]Previous studies have reported the correlation between thin endometrium and infertility [7–10]. Therefore, improving endometrial thickness in patients with thin endometrium will likely benefit pregnancy outcomes in great part. Over the years, several treatment modalities have been suggested for thin endometrium, including hysteroscopic adhesiolysis, hormonal manipulation, and adjuvants (aspirin, luteal oestradiol, sildenafil citrate, granulocyte colony-stimulating factor) [11]. Despite the vast diversity of treating methods, there is only a minor facilitating change reported in the endometrium thickness and implantation rates without robust evidence, especially for severe endometrium-injured patients [11, 12]. Thus, treatment of thin endometrium remains a challenge, and future studies are crucial to improve pregnancy outcomes in patients with thin endometrium.

In the field of cell therapy, stem cell transplantation has pioneered novel approaches for the biomedical treatment of injured endometrium [13, 14]. MSCs are undifferentiated pluripotent stem cells with the characteristics of paracrine, immune regulation, and multi-directional differentiation [15]. The origins of MSCs include autologous bone marrow, autologous peripheral blood, autologous muscle, allogeneic fetal liver, allogeneic umbilical cord, etc. MSCs infusion therapy has been applied in animal models and preclinical experiments of various diseases and has shown favorable outcomes in relieving animal symptoms as well as improving patients' comprehensive signs [15, 16]. For the therapy of thin endometrium, there are only a handful of reported cases hitherto, among which bone marrow-derived mesenchymal stem cells (BM-MSCs)are principally studied, while major focus is on the therapeutic results, yet the underlying mechanism [17]. Besides, several barriers hinder the promotion and application of BM-MSCs in large-scale clinical practice. Firstly, the content of MSCs in bone marrow is quite insufficient in humans, with merely 1/100000 to 1/1000000, which is poorer in elderly donors and patients with bone marrow diseases. Secondly, bone marrow collection is invasive, with an increased risk of microbial infection. In contrast, the placenta is a *bona fide* candidate origin of MSCs. Abundant MSCs have been found in the placenta, which comes from the embryonic mesoderm in common with bone marrow and peripheral blood, and contains large number of MSCs, endothelial progenitor cells, hematopoietic trophoblast, and fibroblasts. Accordingly, HP-MSCs not only have the vigorous expansion ability and low immunogenicity in common with BM-MSCs, but also exhibit advantages of abundance and no harm to the fetus and the mother without ethical restrictions [18, 19]. Besides, recent research indicates that HP-MSCs also show greater proliferation capacity than umbilical cord-derived MSCs (UC-MSCs) [20]. Taken together, HP-MSCs can be considered as a novel alternative source for stem cell therapy.

Physiologically, the uterus is closely interlinked with the vagina. Thus, the traditional *in situ* instillation of HP-MSCs tends to cause part of the cell suspension to slip out of the uterus via the vagina, which limits the maximal efficacy of stem cells retention. Several novel strategies have been adopted for enhancing the retention time of stem cells, including hyaluronic acid (HA) and Pluronic F-127 [21–26]. Among those, HA hydrogel is a promising candidate for the encapsulation and release of HP-MSCs for endometrial therapy. The existence of hyaluronidase in the endometrium can effectively degrade HA, in case that HA stays in the uterine cavity persistently without decomposition [27]. Moreover, HA hydrogel has a three-

dimensional cross-linked network and shows low interfacial tension and adhesion characteristics, which can provide structural and mechanical support for adjacent cells. As a result, HP-MSCs can be gradually released from the hydrogel to achieve the optimal therapeutic effect [24].

The human endometrium is a complex and dynamic tissue that consists of an outer functionalis layer and an inner basalis layer. The functionalis is composed of compact glandular tissue and a slack connective stroma, while the inner basalis layer contains mainly stroma [28]. The endometrial undergoes morphological and secretory changes during the menstrual cycle, which are critical for uterine receptivity. Exploring the effects of HP-MSCs on endometrial regeneration might help us to improve cell therapy for thin endometrium.

In the present study, we encapsulate the HP-MSCs within a HA hydrogel(HP-MSCs-HA)and then evaluate the therapeutic effects of HP-MSCs-HA on the murine model of thin endometrium *in vivo*, including the embryo implantation rate, the endometrial thickness, the number of glands, the degree of fibrosis, and the proliferation promoting effect. Furthermore, we probe the potential molecular mechanism and signal pathway of HP-MSCs on endometrial stromal and glandular cells *in vitro*.

Methods

Materials

Hyaluronic acid (HA, 97%) and glycidyl methacrylate (GMA, 98%) were purchased from Maclin Biochemical Co. Ltd and J&K Chemical Ltd, respectively. 2-hydroxy-4'-(2-hydroxyethyl)-2-methylpropiophenone (Photoinitiator Irgacure 2959, 99%) was obtained from Aladdin Bio-Chem Technology Co. Ltd. All chemicals were used as received without further purification.

Identified HP-MSCs were kindly provided by the College of Life Sciences-iCell Biotechnology Regenerative Biomedicine Laboratory, Zhejiang University. The identification results of these HP-MSCs were provided in supplement materials. The cells were cultured in basic DMEM/F12 medium (Hyclone, Logan, UT, USA) containing 10% fetal bovine serum (FBS, Biological Industries, Kibbutz Beit-Haemek, Israel), 1% penicillin (Geno, Hangzhou, China) at 5% CO_2 and 37 ^{o}C as previously optimized [29, 30].

Preparation and characterization of HA hydrogel

The polymerizable HA was prepared via the chemical modification of HA by using GMA, as shown in Figure 1A. Briefly, 0.5 g HA was dissolved in 100 mL mixture of *N, N*-dimethylformamide (DMF), and phosphate buffer saline (PBS) solution (0.01 M, pH = 7.40) with a volume ratio of 1:1 overnight. The mixture was subsequently mixed with 3.35 g of triethylamine (TEA) for 30 min. Then, 6.65 g GMA was added to the mixture and stirred for 5 days at room temperature. The reaction mixture was precipitated in 20 times excess acetone solution. The precipitates were collected and dried in a vacuum oven. The products were purified by dialysis in deionized water for 3 days and further dried by lyophilization, leading

to the final GMA functionalized HA powders, coded as GM-HA. To prepare HA hydrogel, 10 mg GM-HA were dissolved in 1 mL aqueous solution containing 1‰ Irgacure 2959 photoinitiator. The mixed solution was then exposed to 365 nm UV light for 15 min, leading to the formation of HA hydrogels.

^{1}H-NMR spectrum of GM-HA was recorded on a 400 MHz Bruker NMR instrument with D_2O as a solvent. Fourier transform infrared (FT-IR) spectra of GM-HA and HA hydrogel were obtained by a Bruker Vector 22 spectrometer. The rheological measurement of HA hydrogel was carried out on DHR2-2183 rheometer at 37 ^oC. The morphologies of HA and HA hydrogel were observed by Nova Nano scanning electron microscopy (SEM 450, Thermo FEI). The HA and lyophilized HA hydrogel power were evenly spread on the conductive glue and purged three times with an ear wash ball for SEM samples. The prepared samples were sprayed with platinum for 60 s before SEM observation. After that, 500 μL HA hydrogel was mixed with 4 ´10^6 HP-MSCs and incubated at 37 °C for 10 min to prepare HP-MSCs-HA, and the mouse was injected with 25 μL HP-MSCs-HA per uterus.

Isolation and culture of Human stromal and glandular cells

A total of 20 female patients aged between 24-48 years old with normal menstrual cycles (21-35 days) were recruited at Women's Hospital of Zhejiang University, China. They haven't received hormone therapy at least three months before surgery. All the patients underwent hysteroscopy and endometrial biopsy during the infertility examination. Stromal and glandular cells were isolated from the endometrium as previously described [31]. Both groups of cells were cultured in DMEM/F12 medium containing 10% FBS and 1% Penicillin-Streptomycin at 37 ^oC in a humidified environment with 5% CO_2. After coculturing with HP-MSCs for 24 h, 48 h, 72 h, respectively, the cells were used to measure EdU/Transwell/Western blot assay.

In vivo tracing of CM-DiD/CM-DiR-labeled HP-MSCs

The commercial cell membrane red fluorescent probe CM-DiD/CM-DiR (US Everbright® Inc, Jiangsu, China) was diluted with DMSO according to the manufacturer's instructions to make a final concentration of 1 mM. HP-MSCs at a density of 10^6 cells/mL were suspended in 5 mL PBS. 10 μL CM-DiD or CM-DiR cell-labeling solution was then added at 37 °C for post-instillation tracking in utero. After 20 min, the labeled cells were spun at 800 x g for 3 min and followed with washing twice with 5 mL PBS at 1000 x g for 5 min each. The CM-DiD and CM-DiR labeled HP-MSCs were then mixed with as-prepared HA hydrogel, respectively, to form two HP-MSCs-HA with different fluorescent labels. The mouse model was divided into two groups, as shown below, one group was injected with CM-DiR labeled HP-MSCs and HP-MSCs-HA for imaging, using an IVIS Spectrum to detect after transplantation for 1, 3, 7, 14, and 35 days, respectively. The other group was injected with CM-DiD label HP-MSCs and HP-MSCs-HA, which was used for the frozen section. Slides with 6 μm thick (cutting with a CryoStar NX50, Thermo) were observed by an Olympus IX81-FV1000 fluorescence microscope.

CM-DiR labeled group:

Left uteri: instillation of HP-MSCs alone (coded as HP-MSCs)

Right uteri: instillation of HP-MSCs-HA (coded as HP-MSCs-HA)

CM-DiD labeled group:

Left uteri: instillation of HP-MSCs alone (coded as HP-MSCs)

Right uteri: instillation of HP-MSCs-HA (coded as HP-MSCs-HA)

Transwell migration assay

Human stromal cells or glandular cells were cultured in the upper plate compartment (8-μm, 24-well insert, Corning, NY, USA), while the HP-MSCs were cultured in the lower chamber. They were then cocultured at 37 ^{O}C for 24 h, 48 h, and 72 h, respectively. The medium and cells were then removed from the upper chamber using cotton swabs with 1×PBS, while the migrated cells on the bottom surface of the membrane were fixed and stained with 0.5% crystal violet [32]. Cells from 5 random fields were counted using an inverted microscope with a magnification of 200x.

EdU proliferation assay

Human stromal cells or glandular cells were plated in 24-well plates and cocultured with HP-MSCs which were in the upper insert (0.4-μm, 24-well insert, Corning, NY, USA). After incubated for 24 h, 48 h, and 72 h, respectively, the transwell insert loaded with HP-MSCs were removed, and cell proliferation activity was assessed using a commercially available EdU Assay Kit (RIBOBIO, Guangdong, China) according to the protocol provided. Cell proliferation was quantified by the incorporation of EdU into the newly synthesized DNA of replicating cells. The proliferated cells were dyed red, while the nuclei of all cells were dyed blue with DAPI. By counting EdU/DAPI ratio, cell proliferation ability can be assessed.

Protein isolation and western blot analysis

Proteins were extracted from the treated human endometrial stromal cells and glandular cells and then lysed by RIPA lysis buffer (Cell Signaling Technology, Boston, MA, USA) as previously described [24]. The concentration of protein was detected using a bicinchoninic acid protein assay kit (Thermo Scientific, Waltham, MA, USA). Proteins were denatured in a 5× SDS-PAGE loading buffer (CWBIO, Beijing, China). Then they were separated on sodium dodecyl sulfate-polyacrylamide gels and subsequently transferred onto nitrocellulose membranes. After being blocked with 5% BSA (Albumin from bovine serum) in PBS, the membranes were incubated with primary and secondary antibodies. The immunoblots were washed with PBST (PBS with 0.1% Tween-20). And then the membranes were incubated overnight with primary

antibodies at 4^{o}C. After washing, secondary antibodies were added and incubated at room temperature for 1 h in the dark. Finally, the membranes were probed with an Odyssey CLx (LI-COR, USA). The signal intensity was calculated with ImageStudio. Protein expression was normalized to β-Actin.

Rabbit monoclonal anti-p-JNK (9255), rabbit monoclonal anti-JNK (9252), rabbit monoclonal anti-p-Stat3 (9145), mouse monoclonal anti-Stat3 (9139), rabbit monoclonal anti-p-Erk1/2 (4370), rabbit monoclonal anti-Erk1/2 (4695), rabbit monoclonal anti-p-Jak2 (3771), rabbit monoclonal anti-Jak2 (3230), rabbit monoclonal anti-Stat5 (D3N2B), rabbit monoclonal anti-p-c-Fos (5348), rabbit monoclonal anti-c-Fos (2250), rabbit monoclonal anti-p-c-Jun (3270), and rabbit monoclonal anti-c-Jun (9165) were purchased from Cell Signaling Technology. Mouse monoclonal anti-β-Actin (sc-47778) was purchased from Santa Cruz. Rabbit monoclonal anti-VEGF (GTX102643) was purchased from Gene Tex. Goat anti-mouse fluorescent antibody (926-68020) and Goat anti-rabbit fluorescent antibody (926-32211) were purchased from LI-COR (USA).

Establishment of the endometrium-injured mouse model

8-week-old female ICR mice of clean grade (SLAC company, Shanghai) were reared in the animal center under controlled conditions (21-24 ^{o}C, relative humidity 40-60%, 12 hours light / 12 hours dark cycle), with free access to food and water. To mimic endometrial injury in the clinical setting, we established a mouse model of thin endometrium by both mechanical and chemical injury at the estrous period. Briefly, the surgery involves mechanical intrauterine operation with a syringe contacting with the uterine cavity, as well as chemical injury by intrauterine perfusion with ethanol(95%) [33-35]. The mice were randomly assigned into five groups: sham-operated (PBS) group I, of which the uterine cavity was injected with 25 μL PBS and hold for 3 min; ethanol group II, for which 25 μL 95% ethanol was injected into the uterine cavity to induce damage for 3 min followed with PBS treatment; HA-treated group III, administration of HA after endometrium damage by 25 μL 95% ethanol as described above; HP-MSCs-treated group IV, administration of HP-MSC after endometrium damage by 25 μL 95% ethanol; and HP-MSCs-HA-treated group V, administration of HP-MSCs-HA after endometrium damage by 25 μL 95% ethanol. After acclimation for 7 days, the mice were sacrificed for further analyses. **Figure S1** showed the construction and treatment procedure of the endometrium-injured mouse model in eight steps, which were briefly described as followings: I: mouse anesthesia; II: shaving the back of mouse; III: disinfecting exposed areas; IV: uteri exposure; V: instilling 25 μL ethanol in uterine cavity and holding 3 min to fully establish the model of thin endometrium; VI: intrauterine instillation of treating materials; VII: muscle suture; and VIII: closure of back skin incision.

Histological analysis and immunohistochemistry

Standard H&E staining was used for murine endometrial assessment. 30 treated female mice (6 mice, 12 uteri in each group) were euthanized on day 7 after surgery. The isolated uteri were embedded in paraffin after fixing with 4% paraformaldehyde overnight. The wax blocks were cut into 3-4 μm thick and stained

with Hematoxylin-Eosin staining by standard methods to observe the endometrial thickness and the number of glands. Light microscopy photographs (OLYMPUS VS200, Japan) and endometrial images were analyzed using the Application Program Image Pro-Plus (version 6.0). Endometrial area and perimeter were recorded to assess an average measurement of the endometrial thickness (mean endometrial thickness = area/perimeter). Tissue sections were also labeled with Masson's trichrome to measure the degree of endometrial fibrosis by conventional methods. The area of fibrosis was quantified by measuring the area ratio between endometrial stromal fibrosis and the endometrial area using a quantitative image analysis system (Image-Pro Plus software; Media Cybernetics, Bethesda, MD). The immunofluorescence staining was conducted as previously described [31]. Sections were incubated with primary antibodies Ki67, a rabbit polyclonal primary antibody (ab16667; 1:200; Abcam, Cambridge, UK). The secondary antibody (GK600711; DakoCytomation, Glostrup, Denmark) was applied for 30 min at room temperature. The number of positive staining cells in the glands and stroma was semi-quantitatively scored by the immune response score (IRS) of two observers who did not know the source of the samples. The scoring criteria were the same as previously described [31].

Fertility assessment

40 treated female mice (8 mice in each group) were mated with fertile males of the same age (female: male = 1:1) 7 days after surgery. The female mice were checked for vaginal plugs the next morning to determine whether pregnancy occurred. On the seventh day after the initial detection of vaginal plugs, the mice were sacrificed and the location and number of embryo implantation were recorded by photography.

Statistical analysis

All results were presented as mean ± SEM. We compared the means of samples using student's t-test between two groups and one-way analysis of variance (ANOVA) test among multiple groups. *P*-value < 0.05 was considered statistically significant.

Results

Fabrication and characterization of HA hydrogel

As shown in Fig. 1A, the polymerizable GM-HA was prepared by the ring-opening reaction between HA and glycidyl methacrylate in PBS/DMF solution. Figure 1B showed the ^{1}H-NMR spectrum of GM-HA with D_2O as the solvent, of which the peaks of ~ 5.72 and ~ 6.16 ppm can be assigned to the vinyl protons of methacrylate. Besides, the peaks of ~ 1.93 and ~ 2.00 ppm represented the methyl protons of methacrylate and acetamide in GM-HA, respectively. The degree of methacrylation in GM-HA was estimated to be about 29% according to the ratio of integrated intensity between methacrylate protons and methyl protons in GM-HA acetamide. Figure 1C demonstrated the fabrication and instillation process of HP-MSCs-HA for endometrial therapy. The injectable HA hydrogel was prepared by the

photocrosslinking of 1% GM-HA aqueous solution with 1‰ photoinitiator under UV (365 nm) irradiation for 15 min. The HP-MSCs were then encapsulated by HA hydrogel by uniformly mixing HP-MSCs with HA hydrogels, leading to the formation of HP-MSCs-HA. Figure 1D showed the FT-IR spectra of GM-HA and HA hydrogel. The absorption peak at 1630 cm^{-1} was attributed to the carbon-carbon double bond of methacrylate group. For HA hydrogel, a new absorption peak at 1250 cm^{-1} appeared, which can be assigned to the ether group next to the benzene ring of Irgacure 2959. After crosslinking reaction of the carbon-carbon double bond, the absorption intensity at 1630 cm^{-1} clearly decreased. The characteristic peaks of HA mainly contained the stretching vibrations of pyranose ring, glycosidic linkage, amide, ester, -OH, and -NH groups. Among them, the peaks near 2900 cm^{-1} and 1400 cm^{-1} were belonging to the stretching vibrations of C-H and bending vibrations of $-CH_2$, respectively. The peaks of the pyranose ring and glycosidic linkage can be observed around 1050 cm^{-1}. The broad peak between 3250 cm^{-1} to 3500 cm^{-1} was the typical O-H and N-H stretching vibrations. The peaks at 1550 cm^{-1} to 1700 cm^{-1} can be attributed to the amide and ester groups. The rheology measurements were performed to verify the formation of hydrogel. Figure 1E described the storage modulus (G') and loss modulus (G") of HA hydrogel as a function of oscillation frequency at 37 ^{o}C, which reflected the elasticity and viscosity of the hydrogel, respectively. It is shown that G' of HA hydrogel was larger than the corresponding G" in the oscillation frequency range of 0.01 to 100 rad/s, indicating that the elasticity of HA hydrogel dominates over its viscosity, which can guarantee the retention and coverage of HA hydrogel in the uterine cavity. The morphologies of HA and HA hydrogel were further observed by SEM. Figure 1F indicated that HA did not have a homogeneous structure. However, the cross-linked HA hydrogel exhibited a porous and unbroken skeleton, as shown in Fig. 1G, which can thus facilitate the encapsulation and transportation of small molecules or cells.

The retention time of HP-MSCs in the endometrium

To achieve optimization of therapeutic efficacy, HP-MSCs-HA was fabricated in the present work to promote the enrichment and maximization of the retention of HP-MSCs in the uterus. Prior to *in vivo* experiments, we studied the kinetics of the HP-MSCs being released from the cross-linked HA hydrogel in murine uterine cavities. Unlike humans with solely one inverted pear shape uterus, there are two tubular uteri of mice, closely interlinked with the vagina. The endometrium-injured mouse model was constructed as described in the experimental section. Then, as shown in Fig. 2A, surgical instillation to uterine cavity was adopted to provide stem cell *in situ* therapy. The left uteri of the endometrium-injured mouse model were then given with instillation of HP-MSCs, whereas the right uteri were injected with HP-MSCs-HA. The HP-MSCs were labeled with two fluorescent-labeled fuels, CM-DiD and CM-DiR, respectively. CM-DiD labeling (ex/em: 644/663) was used to track HP-MSCs by *ex vivo* frozen section while CM-DiR labeling (ex/em: 748 /780) was suitable for detecting HP-MSCs by *in viv*o imaging. The *in situ* retention of CM-DiR labeled HP-MSCs was observed by an IVIS Spectrum Imaging System at different time points (1, 3, 7, 14, 28, and 35 days, respectively) after transplantation. Figure 2B-C illustrated HA hydrogel prolonged the retention time of HP-MSCs at every checkpoint and showed significant differences on day 1 (20120000 ± 4640589 p/s vs. 39525000 ± 468817 p/s, $P < 0.01$). Besides, on day 7, the left uterus had few CM-DiR

labeled HP-MSCs, while the right uterus injected with HP-MSCs-HA still had obvious HP-MSCs retention, which indicated that the HP-MSCs can stay in the uterus of sexually mature mice for about two estrus cycles. An *ex vivo* frozen section of the uteri was also conducted to further confirm this. As shown in Fig. 2D, the number of HP-MSCs decreased less slowly and exhibited better extension in the HP-MSCs-HA treated group, which was consistent with the results of *in vivo* imaging. Besides, these results also indicated that HP-MSCs can infiltrate and distribute in the functional layer and basal layer of endometrium, which was beneficial to the regeneration and repair of endometrium.

In vivo therapy of endometrium-injured mouse model with HP-MSCs-HA

The *in vivo* endometrial repair effect of HP-MSCs-HA was thus investigated on the endometrium-injured mouse model established by ethanol perfusion to mimic endometrial injury in real clinical infertile patients. The *in vivo* embryo implantation rate and histological analysis of endometrium, including thickness and gland number, degree of fibrosis, and proliferation effect, were systematically studied.

Embryo implantation refers to the process of early embryo attachment and invasion of the endometrium. In humans, this process begins at the end of the first week after fertilization and endures until the second week of embryo development [36]. Successful embryo implantation requires a receptive endometrium, which allows the uterus to support the development of the embryo and fetus. Therefore, the status of the endometrium can be estimated by measuring the implantation rate of mouse embryos. As shown in Fig. 3A, the 6–8 weeks old ICR mouses were treated with *in situ* instillation of 25 μL of 90% ethanol into the uterine to establish the endometrium-injured model. Correspondingly, a control mouse group injected with the same amount (25 μL) of PBS was also set, which was marked as PBS, as shown in Fig. 3B. The endometrium-injured mice were then divided into four groups randomly and were subjected respectively to PBS, HA hydrogel, HP-MSCs, and HP-MSCs-HA injection into the injured uterine. The mice groups treated with PBS, HA hydrogel, HP-MSCs, and HP-MSCs-HA were coded as Ethanol, HA, HP-MSCs, and HP-MSCs-HA, respectively (Fig. 3B). One week after surgery, some of the mice were mated with normal male mice in order to observe the embryo implantation rate. Figures 3B-C showed that the Ethanol group exhibited a remarkable reduction in the number of the implanted embryo as compared to that of the PBS group. The average number of fetuses developed in the Ethanol group was 3.273 ± 0.506, which is approximately half of the PBS group (7.154 ± 0.478), confirming the successful establishment of the endometrium-injured model. The HA group (4.538 ± 0.447) did not show prominent difference in the number of fetuses as compared with that of the Ethanol group, while the HP-MSC (4.917 ± 0.621) and HP-MSCs-HA group (5.889 ± 0.539) developed a significantly higher number of fetuses as compared with that of the Ethanol group. These results indicated that HP-MSCs-HA achieved the best therapy outcome by prolonging their retention time in the uterine cavity.

Maintaining sufficient endometrial thickness is a precondition for endometrial receptivity and implantation. Patients with thin endometrium have fewer glandular cells than the normal thickness group [3]. H&E staining was applied to evaluate the endometrium thickness as well as the gland number in each group of mice one week after surgery. As shown in Fig. 4A, the Ethanol group showed thinner endometrial

thickness and fewer endometrial glandular cells as compared with those of the PBS group. After treatment, the most effective endometrial regeneration was observed in the HP-MSCs-HA group, in which their endometrium presented a well-organized structure with epithelia and secretory glands. Besides, the thickness of the endometrial layers in the HP-MSCs-HA group was up to 292.3 ± 19.14 μm, which was approximately twice as thick as that of the Ethanol group (171.3 ± 14.59 μm) **(**Fig. 4D**).** As shown in Fig. 4E, the number of glandular cells was also significantly improved by HP-MSCs-HA treatment.

One of the commonly described causes of thin endometrium is asherman syndrome (intrauterine adhesions), which is characterized by injury to the basal layer of the endometrium, leading to endometrial fibrosis[3, 37, 38]. Masson staining was further used to analyze the fibrous area and the collagen in order to evaluate the level of intrauterine adhesions. The images in Fig. 4B and Fig. 4F revealed that the Ethanol group presented higher fibrous tissue (blue) contents of 0.477 ± 0.027 than those of PBS group (0.245 ± 0.017), HA-group (0.374 ± 0.027), HP-MSCs group (0.289 ± 0.019), and HP-MSCs-HA groups (0.279 ± 0.016). The HP-MSCs and HP-MSCs-HA group exhibited significant therapeutic outcomes, in which the fibrosis area was not significantly different from that of the PBS group. Additionally, HA hydrogel alone can also restore fibrosis to some extent but is less effective than stem cell treatment.

The proliferation of endometrial cells can be assessed by immunohistochemical staining of Ki67, which can label the cells in the cell cycle. Figure 4C showed the proliferation of endometrial cells and stromal cells by the immunohistochemical staining of Ki67 for the five groups. As shown in Fig. 4G, the IRS scores of ki67 in PBS, Ethanol, HA, HP-MSCs and HP-MSCs-HA groups were 4.743 ± 0.745, 2.008 ± 0.306, 3.201 ± 0.427, 4.104 ± 0.369, 4.319 ± 0.527, respectively. The RIS of Ki67 in the Ethanol group was significantly lower than that of the PBS group. Whereas, the HP-MSCs and HP-MSCs-HA group presented an expression of Ki67 close to that of the PBS group.

These *in vivo* experimental results indicated the safety and effectiveness of HP-MSCs-HA used for treating thin endometrium in the mouse model.

Effects of HP-MSCs on the proliferation and migration of human endometrial stromal cell

Based on the therapeutic results, further studies remain to uncover the underlying molecular mechanism. The stromal and glandular cells were thus isolated from the human endometrium to investigate the bioactive effects of HP-MSCs on them *in vitro*, as described in the experimental section. The obtained human primary endometrial stromal and glandular cells were identified by immunohistochemical staining of CK7 and Vimentin, as shown in **Figure S2**. Besides, Fig. 5 illustrated the proliferation effect of HP-MSCs on human stromal cells. The human endometrial stromal cells were cultured without or with HP-MSCs for 24 h, 48 h, and 72 h, respectively, before EdU exposure. EdU/DAPI was the ratio of proliferating cells to total cells that can be used to evaluate cell proliferation. The proliferation rates of stromal cells without and with the presence of HP-MSCs were 14.34 ± 1.492% vs. 23.64 ± 1.795% at 24 h, 18.85 ± 1.358% vs. 25.18 ± 1.456% at 48 h, 25.86 ± 4.657% vs. 45.5 ± 4.442% at 72 h, respectively (Fig. 5A-C,

Fig. 5E-G), confirming that the proliferation ability of stromal cells was significantly enhanced by HP-MSCs.

The effect of HP-MSCs on the migration of human endometrial stromal cells was also conducted. The stromal cells were cultured without (Ctr group) and with HP-MSCs (HP-MSCs group) for 24 h, 48 h, and 72 h, respectively, which were then analyzed by a transwell assay, as shown in Fig. 6A. The numbers of the migrated stromal cells in the HP-MSCs cocultured group at 24 h and 48 h significantly exceeded that in the corresponding control group (Ctr) without HP-MSCs, as shown in Fig. 6B. However, at 72 h, a minor difference in the number of migrated stromal cells can be observed between the Ctr and HP-MSCs groups. With quantification, the migration rate of stromal cells of the Ctr and HP-MSCs groups were significant as 11.6 ± 1.691% vs. 66.4 ± 1.435% at 24 h and 84.3 ± 6.391% vs. 175.3 ± 4.807% at 48 h (Fig. 6C), indicating that HP-MSCs not only benefited the proliferation of human endometrial stromal cells but also promoted their migration.

Given the cellular effects of HP-MSCs on endometrial stromal cells, the underlying mechanisms were further explored via western blot. Figure 6D showed that coculturing with HP-MSCs can significantly promote the expression of VEGF and the phosphorylation level of JNK, Erk1/2, and Stat3 at 24 h. Besides, elevated expression of p-JNK, p-Stat3, and VEGF could be observed until 48 h compared to those of the control group. Hence with the above results, it can be concluded that coculturing with HP-MSCs exhibited beneficial effects on the proliferation and migration of human endometrial stromal cells via the JNK/Erk1/2-Stat3-VEGF pathway *in vitro*.

Effect of HP-MSCs on the proliferation of human endometrial glandular cell

In addition to stromal cells, endometrial glandular cells are the other essential component of the endometrium. Similarly, HP-MSCs were cocultured with the glandular cells for 24 h, 48 h, and 72 h, respectively, and then examined by EdU assay (Fig. 7D). As shown in Fig. 7A-C, the proliferation rates of the HP-MSCs group and the basal medium group at 24 h, 48 h, and 72 h were 2.842 ± 0.463% vs. 4.278 ± 0.463%, 5.203 ± 0.559% vs. 5.561 ± 0.988%, 8.485 ± 0.562% vs. 10.94 ± 1.488%, respectively, which indicated that HP-MSCs can promote the proliferation of human endometrial glandular cells at 24 h (Fig. 7E). However, no significant differences were observed at 48 h and 72 h (Fig. 7F-G).

We further investigated the potential mechanisms of such proliferation enhancement via western blot. As shown in Fig. 7H, the results of western blot validated that HP-MSCs can activate the phosphorylation of c-Fos and upregulate the expression of VEGF protein at 24 h. Besides, elevated expression of p-Jak2 and p-Stat5 were also observed after exposure to HP-MSCs for 24 h. Taken together, these results proved that HP-MSCs coculturing can improve the migration of human endometrial glandular cells via the Jak2-Stat5 and c-Fos-VEGF pathway, providing favorable conditions for endometrial repair.

Discussion

In this study, we demonstrated a novel strategy to improve the thickness of mouse thin endometrium by HP-MSCs cross-linked with HA hydrogel. HP-MSCs-HA could retain in the endometrium to promote the proliferation, migration of stromal cells and glandular cells, thereby improving embryo implantation rates.

Recent studies had shown that MSCs could serve as a therapeutic agent for thin endometrium caused by endometrial injury [13, 14]. Though MSCs are commonly found in bone marrow, umbilical cord, fat tissue, and amniotic membrane, they are difficult to obtain for large-scale clinical applications owing to the limited sources and invasively collecting methods. HP-MSCs represent an emerging alternative source for tissue regeneration. HP-MSCs are advantageous over other MSCs for a variety of reasons, such as their robust expansion ability, superior safety profile as well as extensive sources. Noticeably, HP-MSCs can be directly applied to mouse models without immune response due to the low immunogenicity [39–41]. These advantages of HP-MSCs make them the ideal source for cell therapy. Interestingly, HP-MSCs were also found to improve angiogenesis, trigger regeneration of damaged organs [38]. Our findings suggested that HP-MSCs are an effective way for treating injured endometrium via rescuing the dysfunctional stromal healing response, progressive fibrosis, and poor vascular development. These suggest that HP-MSCs based therapy is a potential therapeutic approach.

Mesh-like HA hydrogel could provide structural and mechanical support for HP-MSCs, and improve their retention time and therapeutic effects. Moreover, HA hydrogel is safe for mice and human, since it can be decomposed by hyaluronidase in endometrium. We found HP-MSCs-HA could infiltrate and distribute both in functional layer and basal layer of endometrium, and retain longer than HP-MSCs. This effect is very likely due to the gradual release of HP-MSCs from the hydrogel. Furthermore, Hooker *et.al* recently found that HA hydrogel therapy seems to improve fertility and reproductive outcomes in women who had experienced at least one previous dilation and curettage, which indicated the extra beneficial characteristic of HA hydrogel on endometrial repair [42, 43]. Thus, HA hydrogel holds great potential as an intrauterine controlled-release delivery system. Our study further confirmed the beneficial aspects of HP-MSCs-HA on endometrial injury repair in mouse model. Although there's no statistical significance on endometrial thickness between HP-MSCs-HA and HP-MSCs group, HP-MSCs-HA instillation significantly decreased the fibrous area and enhanced the proliferation ability of endometrial cells, in contrast to HP-MSCs instillation. This is potential consequence of the shorter menstrual cycle in mice (4–5 days per cycle) than that of humans (28–30 days per cycle). Even without HA, HP-MSCs can stay in the uterus of sexually mature mice for about two estrus cycles. This retention time is sufficient for the repair of endometrium in mice. Besides, HA alone also showed a certain effect on endometrial repair in reducing endometrial fibrosis. However, the profound retention effects of HP-MSCs-HA on humans with thin endometrium need further investigation.

Endometrial repair is closely relevant to physiological and pathological activities such as cell proliferation, differentiation, and migration, and plays an important role in re-epithelialization of the injured endometrium[44]. The ERK1/2 and JNK are two parallel MAPK signaling pathways in response to diverse extracellular stimuli, and they are involved in cell growth, differentiation, apoptosis, and inflammatory response effects [45, 46]. In our study, the protein levels of p-JNK, p-ERK1/2, p-STAT3, and

VEGF were remarkably increased in HP-MSCs-treated endometrial stromal cells, which may partially explain the proliferation and migration-promoting effects of HP-MSCs on stromal cells. Consistent with our findings, evidence has shown that the activation of JNK/Erk1/2-Stat3-VEGF pathway can promote the development of endometrial cells and likely enhance the uterine capacity [47, 48]. Jak2/Stat5 and c-Jun/c-Fos pathway play an important role in cell proliferation and migration. In our study, Jak2-Stat5 and c-Fos-VEGF pathways were up-regulated in glandular cells when coculturing with HP-MSCs, which may account for the increase of gland number in HP-MSCs' treated group.

Conclusions

In this study, HP-MSCs-HA were successfully prepared for the treatment of endometrial injury. HP-MSCs-HA exhibited a prolonged retention time in mouse uterus in contrast to HP-MSCs instillation alone. The *in vivo* therapeutic outcomes of endometrium-injured mouse models proved that HP-MSCs-HA can rescue the injured-endometrium in mice via increasing the thickness and gland number of endometrium, decreasing the fibrous area, and thus improving the implantation rate. The *in vitro* results suggested that HP-MSCs can promote the proliferation of human endometrial stromal through activation of JNK/Erk1/2-Stat3-VEGF pathway, and promote the proliferation and migration of glandular via Jak2-Stat5 and c-Fos-VEGF. Overall, our study provides theoretical and experimental foundations for the clinical treatment of thin endometrium using HP-MSCs-HA.

Abbreviations

ART: Assisted reproductive technologies; BM-MSCs: Bone marrow-derived mesenchymal stem cells; FBS: Fetal bovine serum; FT-IR: Fourier transform infrared; GMA: Glycidyl methacrylate; HA: Hyaluronic acid; HA hydrogel: Hyaluronic acid hydrogel; HCG: Human chorionic gonadotropin; HP-MSCs: Human placenta-derived mesenchymal stem cells; HP-MSCs-HA: HP-MSCs encapsulated within HA hydrogels; Jak2: Janus Kinase 2; MSCs: Mesenchymal stem cells; PBS: Phosphate buffer saline; SEM: Scanning electron microscopy; Stat3: Signal transducer and activator of transcription 3; Stat5: Signal transducer and activator of transcription 5; TEA: Triethylamine; UC-MSCs: Umbilical cord-derived MSCs.

Declarations

Acknowledgements

We thanked the College of Life Sciences-iCell Biotechnology Regenerative Biomedicine Laboratory, Zhejiang University for kindly provided us with identified HP-MSCs.

Authors' contributions

The manuscript was written through the contributions of all authors. ZD and DB designed, organized, and instructed the study. Study concept and design: ZD, DB, LY, DS, YX; Collect the human endometrial samples: LY, YX, LJ, CR, WF, CJ; Perform the experiments: LY, DS, YX, LJ, ZY, YY, NF; Analyze and

interpreted the results: LY, DS, YX, LJ; Draft the manuscript: LY, DS, TM, WS, YX; Revised the manuscript: ZD, DB, LY, DS, YX. All authors have approved the final version of the manuscript.

Funding

This work was supported by the National Key Research and Development Program of China (2018YFC1005003), Zhejiang Provincial Key Research and Development Program (No. 2021C03098), the National Natural Science Foundation of China (No. 81771535 and 21875214), Zhejiang Provincial Key Medical Technology Program (WKJ-ZJ-1826), and the second level of the 2016 Zhejiang Province 151 Talent Project.

Availability of data and materials

The datasets used and/or analyzed during the current study are available from the corresponding author on reasonable request.

Ethics approval and consent to participate

The research protocol was approved by the Ethics Committee of the Women's Hospital of Zhejiang University, China. Written informed consents were obtained from all participants before tissue collection. All animal research, feeding, processing, stem cell instillation, sample collection, and experimental procedures were carried out following the principles and procedures. We confirmed that the human and animal studies in our experiments were carried out under the relevant guidelines and regulations approved by the Women's Hospital of Zhejiang University (IRB-20210054-SC) and Laboratory Animal Center of Zhejiang University (ZJU20210088), China.

Consent for publication

Not applicable.

Competing interests

The authors declare that they have no competing interests.

References

1. Deans R, Abbott J. Review of intrauterine adhesions. J Minim Invasive Gynecol. 2010;17(5):555–69.
2. Cenksoy P, Ficicioglu C, Yıldırım G, Yesiladali M. Hysteroscopic findings in women with recurrent IVF failures and the effect of correction of hysteroscopic findings on subsequent pregnancy rates. Arch Gynecol Obstet. 2013;287(2):357–60.
3. Liu K, Hartman M, Hartman A. Management of thin endometrium in assisted reproduction: a clinical practice guideline from the Canadian Fertility and Andrology Society. Reprod Biomed Online. 2019;39(1):49–62.

4. El-Toukhy T, Coomarasamy A, Khairy M, Sunkara K, Seed P, Khalaf Y, Braude P. The relationship between endometrial thickness and outcome of medicated frozen embryo replacement cycles. Fertil Steril. 2008;89(4):832–9.
5. Tan S-Y, Hang F, Purvarshi G, Li M-Q, Meng D-H, Huang L-L. Decreased endometrial vascularity and receptivity in unexplained recurrent miscarriage patients during midluteal and early pregnancy phases. Taiwanese Journal of Obstetrics Gynecology. 2015;54(5):522–6.
6. Rinaldi L, Lisi F, Floccari A, Lisi R, Pepe G, Fishel S. Endometrial thickness as a predictor of pregnancy after in-vitro fertilization but not after intracytoplasmic sperm injection. Hum Reprod. 1996;11(7):1538–41.
7. Momeni M, Rahbar MH, Kovanci E. A meta-analysis of the relationship between endometrial thickness and outcome of in vitro fertilization cycles. J Hum Reprod Sci. 2011;4(3):130–7.
8. Noyes N, Liu HC, Sultan K, Schattman G, Rosenwaks Z. Endometrial thickness appears to be a significant factor in embryo implantation in in-vitro fertilization. Hum Reprod. 1995;10(4):919–22.
9. Richter KS, Bugge KR, Bromer JG, Levy MJ. Relationship between endometrial thickness and embryo implantation, based on 1,294 cycles of in vitro fertilization with transfer of two blastocyst-stage embryos. Fertil Steril. 2007;87(1):53–9.
10. Liu KE, Hartman M, Hartman A, Luo ZC, Mahutte N. The impact of a thin endometrial lining on fresh and frozen-thaw IVF outcomes: an analysis of over 40 000 embryo transfers. Hum Reprod. 2018;33(10):1883–8.
11. Lebovitz O, Orvieto R. Treating patients with "thin" endometrium - an ongoing challenge. Gynecol Endocrinol. 2014;30(6):409–14.
12. Xie Y, Zhang T, Tian Z, Zhang J, Wang W, Zhang H, Zeng Y, Ou J, Yang Y. Efficacy of intrauterine perfusion of granulocyte colony-stimulating factor (G-CSF) for Infertile women with thin endometrium: A systematic review and meta-analysis. American journal of reproductive immunology (New York, NY: 1989) 2017, 78(2).
13. Yang H, Wu S, Feng R, Huang J, Liu L, Liu F, Chen Y. Vitamin C plus hydrogel facilitates bone marrow stromal cell-mediated endometrium regeneration in rats. Stem Cell Res Ther. 2017;8(1):267–7.
14. Zhang L, Li Y, Guan C-Y, Tian S, Lv X-D, Li J-H, Ma X, Xia H-F. Therapeutic effect of human umbilical cord-derived mesenchymal stem cells on injured rat endometrium during its chronic phase. Stem Cell Res Ther. 2018;9(1):36–6.
15. Andrzejewska A, Lukomska B, Janowski M. Concise Review: Mesenchymal Stem Cells: From Roots to Boost. Stem Cells. 2019;37(7):855–64.
16. Samsonraj RM, Raghunath M, Nurcombe V, Hui JH, van Wijnen AJ, Cool SM. Concise Review: Multifaceted Characterization of Human Mesenchymal Stem Cells for Use in Regenerative Medicine. Stem Cells Transl Med. 2017;6(12):2173–85.
17. Xia L, Meng Q, Xi J, Han Q, Cheng J, Shen J, Xia Y, Shi L. The synergistic effect of electroacupuncture and bone mesenchymal stem cell transplantation on repairing thin endometrial injury in rats. Stem Cell Res Ther. 2019;10(1):244.

18. Park S, Koh SE, Hur CY, Lee WD, Lim J, Lee YJ. Comparison of human first and third trimester placental mesenchymal stem cell. Cell Biol Int. 2013;37(3):242–9.
19. Zhu SF, Zhong ZN, Fu XF, Peng DX, Lu GH, Li WH, Xu HY, Hu HB, He JM, Su WY, et al. Comparison of cell proliferation, apoptosis, cellular morphology and ultrastructure between human umbilical cord and placenta-derived mesenchymal stem cells. Neurosci Lett. 2013;541:77–82.
20. Feng X, Liu J, Xu Y, Zhu J, Chen W, Feng B, Pan Q, Yu J, Shi X, Yang J, et al. Molecular mechanism underlying the difference in proliferation between placenta-derived and umbilical cord-derived mesenchymal stem cells. Journal of cellular physiology. 2020;235(10):6779–93.
21. Weissmann B. The transglycosylative action of testicular hyaluronidase. J Biol Chem. 1955;216(2):783–94.
22. Liu F, Hu S, Yang H, Li Z, Huang K, Su T, Wang S, Cheng K. Hyaluronic Acid Hydrogel Integrated with Mesenchymal Stem Cell-Secretome to Treat Endometrial Injury in a Rat Model of Asherman's Syndrome. Advanced healthcare materials. 2019;8(14):e1900411.
23. Liu F, Hu S, Wang S, Cheng K. Cell and biomaterial-based approaches to uterus regeneration. Regenerative biomaterials. 2019;6(3):141–8.
24. Lin Y, Dong S, Zhao W, Hu K-L, Liu J, Wang S, Tu M, Du B, Zhang D. Application of Hydrogel-Based Delivery System in Endometrial Repair. ACS Applied Bio Materials. 2020;3(11):7278–90.
25. Kim YY, Park KH, Kim YJ, Kim MS, Liu HC, Rosenwaks Z, Ku SY. Synergistic regenerative effects of functionalized endometrial stromal cells with hyaluronic acid hydrogel in a murine model of uterine damage. Acta Biomater. 2019;89:139–51.
26. Yang H, Wu S, Feng R, Huang J, Liu L, Liu F, Chen Y. Vitamin C plus hydrogel facilitates bone marrow stromal cell-mediated endometrium regeneration in rats. Stem Cell Res Ther. 2017;8(1):267.
27. Zhu R, Huang YH, Tao Y, Wang SC, Sun C, Piao HL, Wang XQ, Du MR, Li DJ. Hyaluronan up-regulates growth and invasion of trophoblasts in an autocrine manner via PI3K/AKT and MAPK/ERK1/2 pathways in early human pregnancy. Placenta. 2013;34(9):784–91.
28. Spencer T, Hayashi K, Hu J, Carpenter K. Comparative developmental biology of the mammalian uterus. Current topics in developmental biology. 2005;68:85–122.
29. Zhang K, Chen X, Li H, Feng G, Nie Y, Wei Y, Li N, Han Z, Han Z, Kong D, et al. A nitric oxide-releasing hydrogel for enhancing the therapeutic effects of mesenchymal stem cell therapy for hindlimb ischemia. Acta Biomater. 2020;113:289–304.
30. Yen B, Hwa H, Hsu P, Chen P, Wang L, Jiang S, Liu K, Sytwu H, Yen M. HLA-G Expression in Human Mesenchymal Stem Cells (MSCs) Is Related to Unique Methylation Pattern in the Proximal Promoter as well as Gene Body DNA. Int J Mol Sci 2020, 21(14).
31. Liu J, Ying Y, Wang S, Li J, Xu J, Lv P, Chen J, Zhou C, Liu Y, Wu Y, et al. The effects and mechanisms of GM-CSF on endometrial regeneration. Cytokine. 2020;125:154850.
32. Liu Y, Zhang X, Sun T, Jiang J, Li Y, Chen M, Wei Z, Jiang W, Zhou L. Knockdown of Golgi phosphoprotein 2 inhibits hepatocellular carcinoma cell proliferation and motility. Oncotarget. 2016;7(16):21404–15.

33. 33.
34. Xia L, Meng Q, Xi J, Han Q, Cheng J, Shen J, Xia Y, Shi L. The synergistic effect of electroacupuncture and bone mesenchymal stem cell transplantation on repairing thin endometrial injury in rats. Stem Cell Res Ther. 2019;10(1):244.
35. Xie Y, Tian Z, Qi Q, Li Z, Bi Y, Qin A, Yang Y. The therapeutic effects and underlying mechanisms of the intrauterine perfusion of granulocyte colony-stimulating factor on a thin-endometrium rat model. Life sciences. 2020;260:118439.
36. Wilcox AJ, Baird DD, Weinberg CR. Time of Implantation of the Conceptus and Loss of Pregnancy. N Engl J Med. 1999;340(23):1796–9.
37. Zupi E, Centini G, Lazzeri L. Asherman syndrome: an unsolved clinical definition and management. Fertility sterility. 2015;104(6):1380–1.
38. Yu D, Wong Y, Cheong Y, Xia E, Li T. Asherman syndrome–one century later. Fertility sterility. 2008;89(4):759–79.
39. Na J, Song J, Kim H, Seok J, Kim J, Jun J, Kim G. Human placenta-derived mesenchymal stem cells trigger repair system in TAA-injured rat model via antioxidant effect. Aging. 2020;13(1):61–76.
40. Chen C, Liu S, Chen C, Chen P, Chen C. Human placenta-derived multipotent mesenchymal stromal cells involved in placental angiogenesis via the PDGF-BB and STAT3 pathways. Biol Reprod. 2015;93(4):103.
41. Xie N, Li Z, Adesanya T, Guo W, Liu Y, Fu M, Kilic A, Tan T, Zhu H, Xie X. Transplantation of placenta-derived mesenchymal stem cells enhances angiogenesis after ischemic limb injury in mice. J Cell Mol Med. 2016;20(1):29–37.
42. Hooker AB, de Leeuw RA, van de Ven PM, Brölmann HAM, Huirne JAF. Reproductive performance after the application of hyaluronic acid gel after dilation and curettage in women who have experienced at least one previous curettage: long-term results of a multicenter prospective randomized trial. Fertil Steril. 2018;110(7):1231–8.
43. Igarashi M. A new therapy for pelvic endometriosis and uterine adenomyosis: local effect of vaginal and intrauterine danazol application. Asia Oceania J Obstet Gynaecol. 1990;16(1):1–12.
44. Gargett C, Nguyen H, Ye L. Endometrial regeneration and endometrial stem/progenitor cells. Reviews in endocrine metabolic disorders. 2012;13(4):235–51.
45. Shao Y, Wang C, Hong Z, Chen Y. Inhibition of p38 mitogen-activated protein kinase signaling reduces multidrug transporter activity and anti-epileptic drug resistance in refractory epileptic rats. Journal of neurochemistry. 2016;136(5):1096–105.
46. Sun Y, Liu W, Liu T, Feng X, Yang N, Zhou H. Signaling pathway of MAPK/ERK in cell proliferation, differentiation, migration, senescence and apoptosis. J Recept Signal Transduct Res. 2015;35(6):600–4.
47. Lim W, Bae H, Bazer FW, Song G. Ephrin A1 promotes proliferation of bovine endometrial cells with abundant expression of proliferating cell nuclear antigen and cyclin D1 changing the cell population at each stage of the cell cycle. J Cell Physiol. 2019;234(4):4864–73.

48. Zhou WJ, Hou XX, Wang XQ, Li DJ. Fibroblast Growth Factor 7 Regulates Proliferation and Decidualization of Human Endometrial Stromal Cells via ERK and JNK Pathway in an Autocrine Manner. Reprod Sci. 2017;24(12):1607–19.

Figures

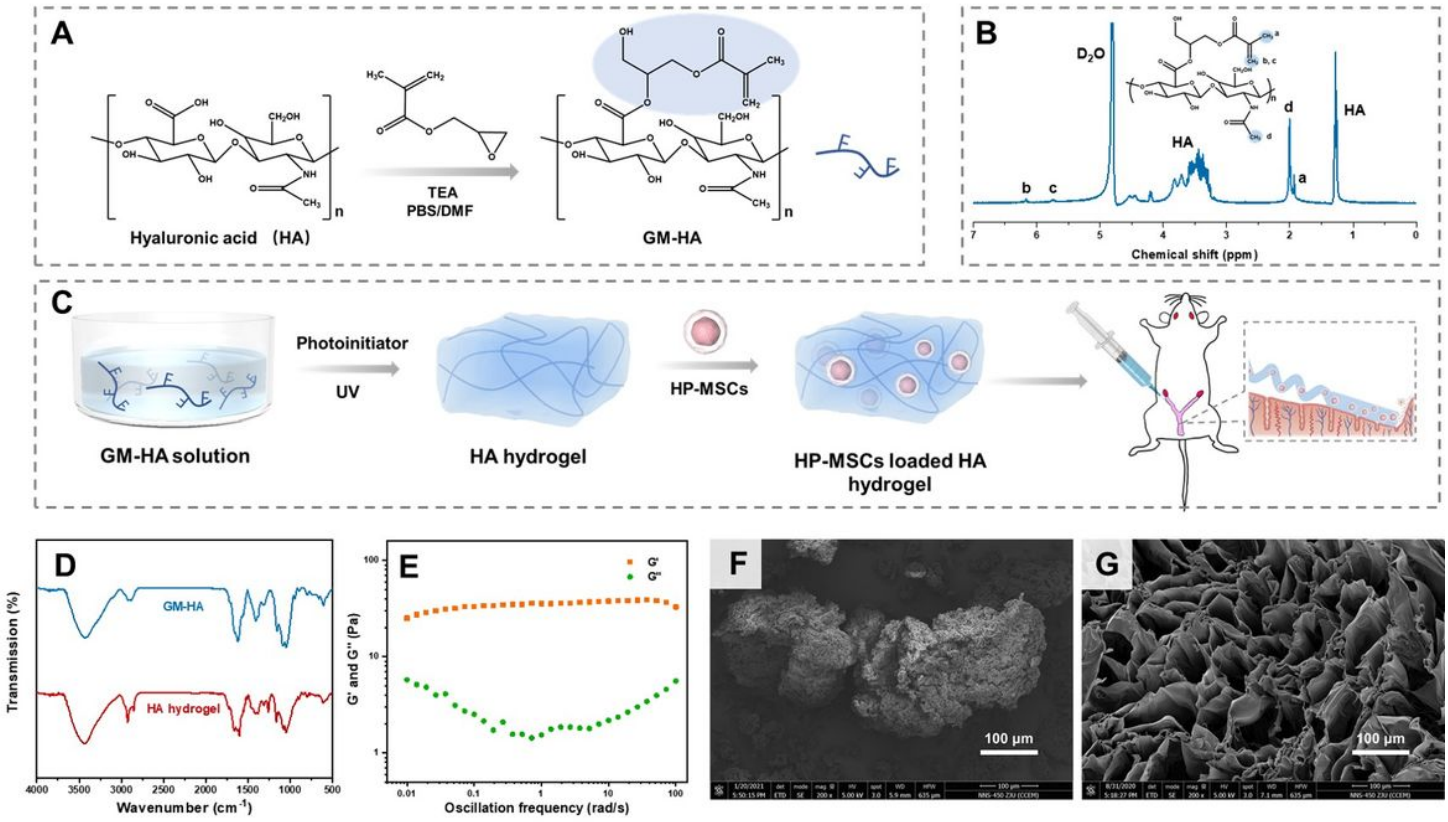

Figure 1

Fabrication and characterization of HA hydrogel. (A) The synthesis routine of GM-HA. (B) The 1H-NMR spectrum of GM-HA in D2O. (C) Schematic presentation of preparation procedures of HA hydrogel and HP-MSCs-HA as well as the instillation of HP-MSCs-HA into a mouse model. (D) The FT-IR spectra of GM-HA and HA hydrogel. (E) The storage modulus G’ and loss modulus G” of HA hydrogel versus oscillation frequency from 0.01 to 100 rad/s with a fixed stain of 0.2% at 37 oC. (F) SEM morphology of freeze-dried HA. (G) SEM morphology of HA hydrogel. The scale bars in (F) and (G) were 100 μm.

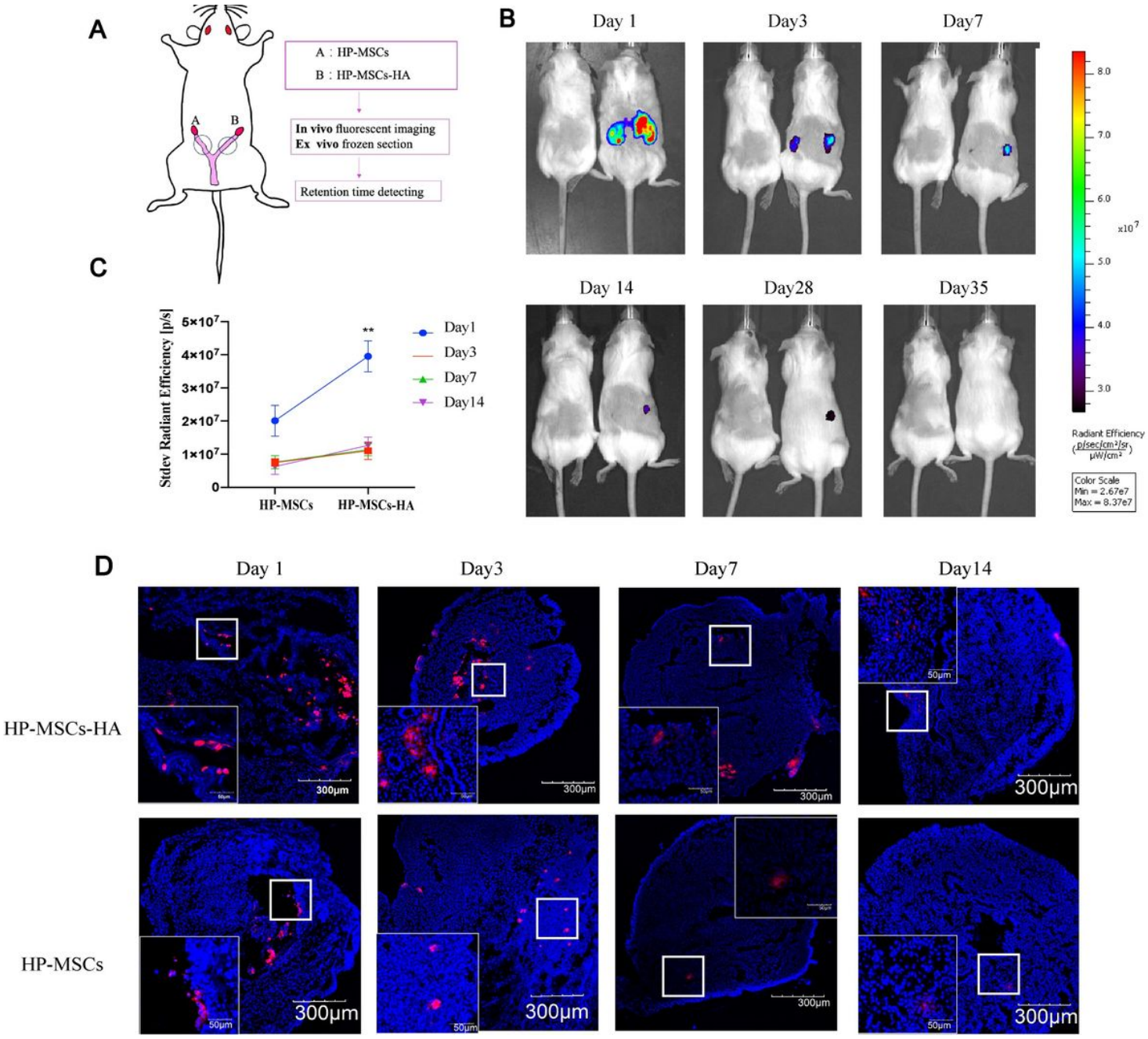

Figure 2

The retention time of HP-MSCs in the endometrium. (A) Schematic presentation of intrauterine instillation and its corresponding detection methods. Equal cell quantities of HP-MSCs and HP-MSCs-HA labeled by CM-DiD or CM-DiR were implanted to the certain uterus (2x105 per/uterus). (B) The mouse on the left was the untreated control group to eliminate the interference of autofluorescence, while the mouse on the right was the treatment group. The retention time of HP-MSCs was observed by an IVIS Spectrum Imaging System at the different time points (1, 3, 7, 14, 28, and 35 days) after transplantation (C) The total radiant efficiency of the treated uterus was measured and calculated. Data were presented as mean ± SEM (n = 3). ** indicates $P < 0.01$. (D) Ex vivo frozen section of the uterus showed the retention of HP-MSCs, which were labeled with CM-DiD (red). The nuclei of cells was labeled with DAPI (blue).

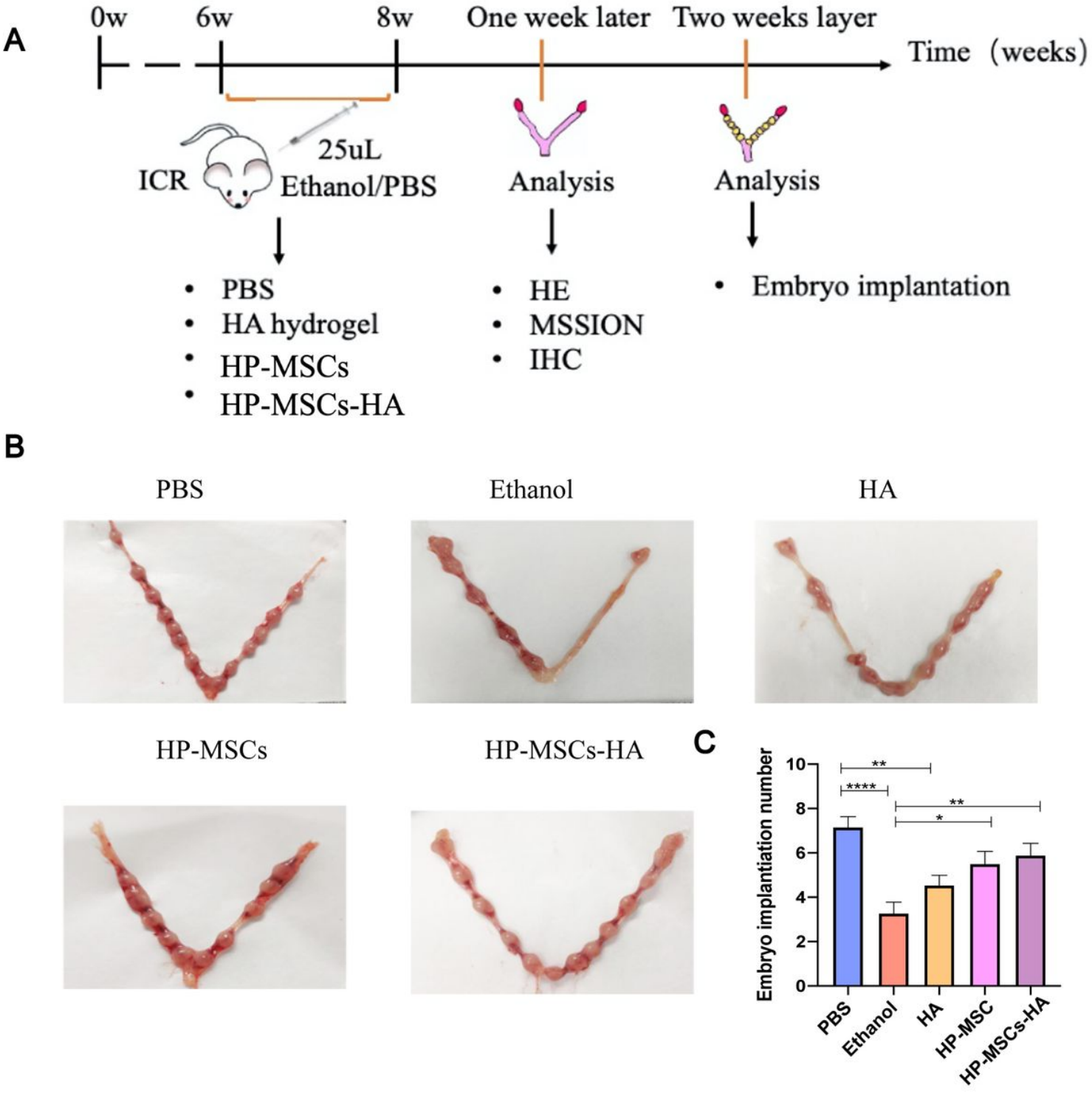

Figure 3

The construction of endometrium-injured mouse model and the evaluation of embryo implantation after therapy. (A) Schematic diagram of mice grouping and their detection methods. (B-C) Evaluate the endometrial receptivity of the five mouse groups with different treatments by the number of implanted embryos. * indicates P <0.05, ** indicates P <0.01, **** indicates P <0.0001, n =8.

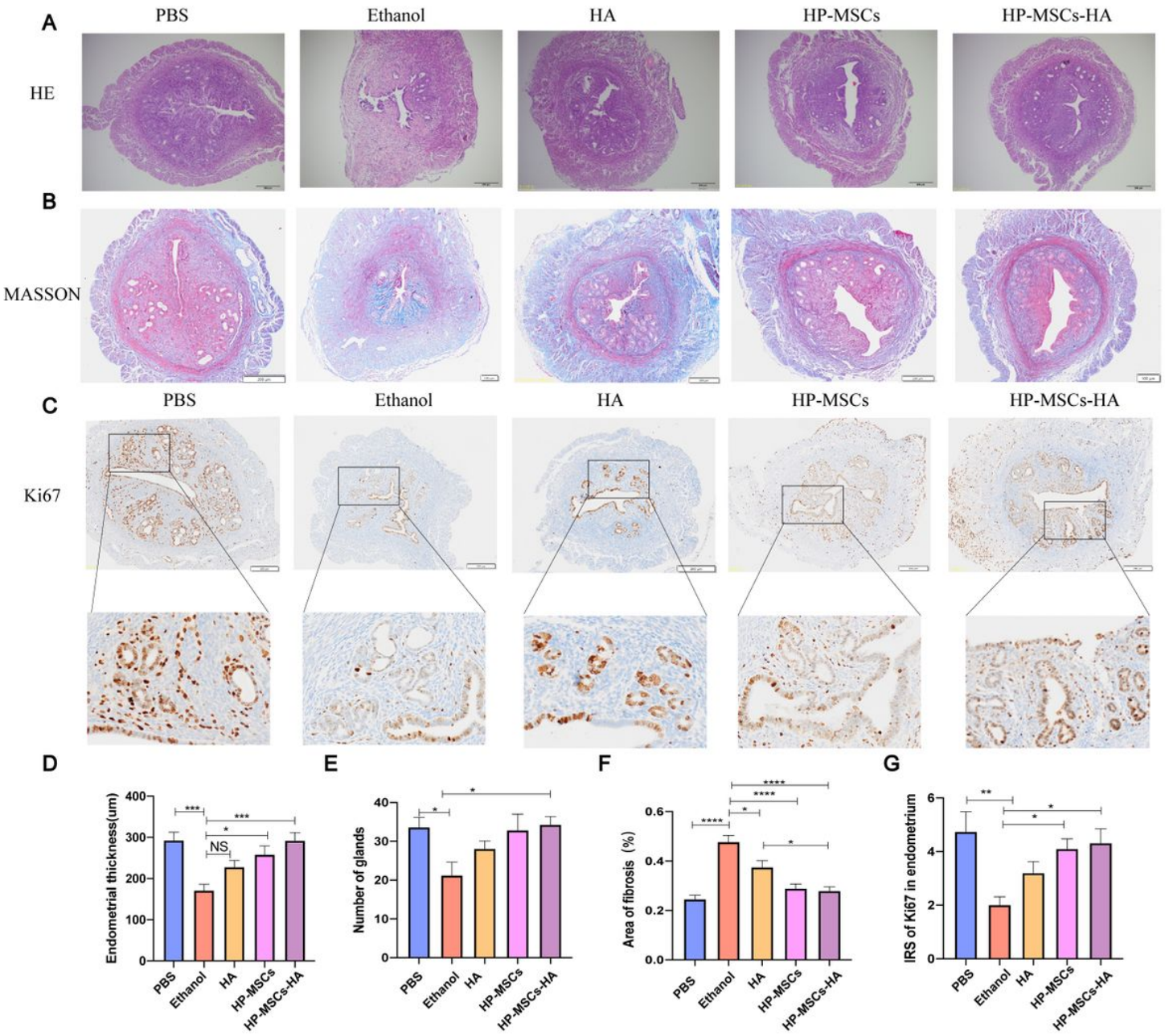

Figure 4

The histological analysis of endometrium for the five mouse groups after different treatments. (A) H&E staining results of the five groups for evaluating the endometrial thickness and number of glands. (B) Masson staining results of the five groups for evaluating the fibrosis status of the endometrium. (C) Immunohistochemical Ki67 expression of the five groups for evaluating the proliferation of endometrial cells and stromal cells. (D) Average endometrial thickness and statistical analysis (±SEM) of the five groups. *indicates P <0.05, *** indicates P <0.001, n=6. (E) Average gland number and statistical analysis (±SEM) of the five groups. * indicates P <0.05, n=6. (F) Average fibrosis area and statistical analysis (±SEM) of the five groups. The ratio of the fibrotic area = endometrial fibrotic area/endometrial area. * indicates P <0.05, **** indicates P <0.0001, n= 6. (G) Statistic analysis of IRS of Ki67 in the endometrium

of the five groups.* indicates P <0.05, ** indicates P <0.01, n=6, *** indicates P <0.001, *** indicates P <0.0001.

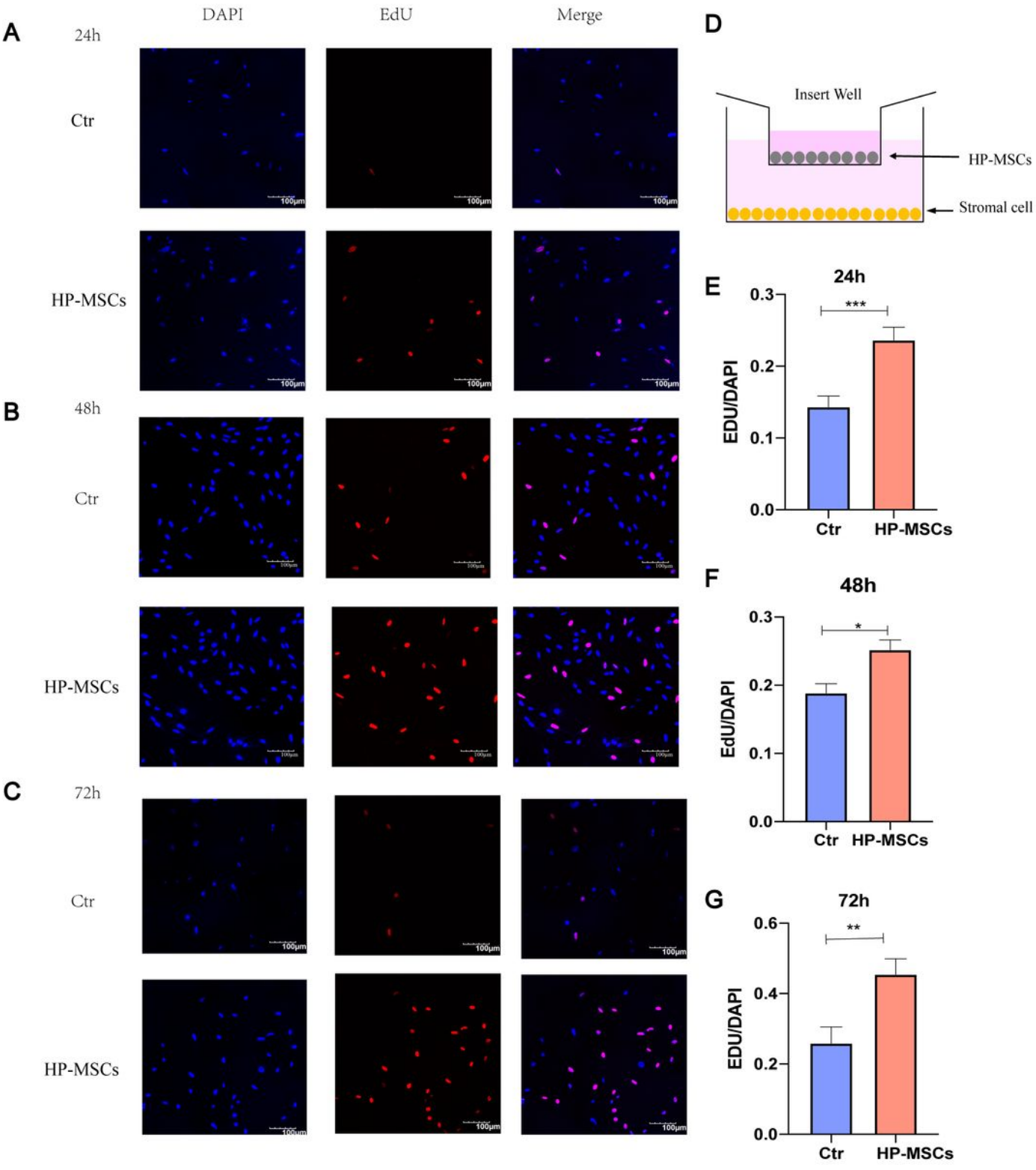

Figure 5

Effects of HP-MSCs on the proliferation of human endometrial stromal cells. EdU assays were conducted at 24 h, 48 h, and 72 h, respectively, after culturing of human stromal cells with (Ctr) and with HP-MSCs, respectively. (A-C) Representative confocal images of human stromal cells stained with EdU (red) and

DAPI (blue) at 24 h, 48 h, and 72 h, respectively. EdU represents the positive proliferation cells while DAPI represents the cell nucleus. (D) Schematic diagram of co-culture, HP-MSCs were inoculated in the upper insert transwell (0.4um), while stromal cells were in the lower hole plate. (E-G). EdU/DAPI represented the ratio of proliferating cells to total cells, and the data were shown as mean ± SEM. *indicates P < 0.05, **indicates P < 0.01, ***indicates P < 0.001.

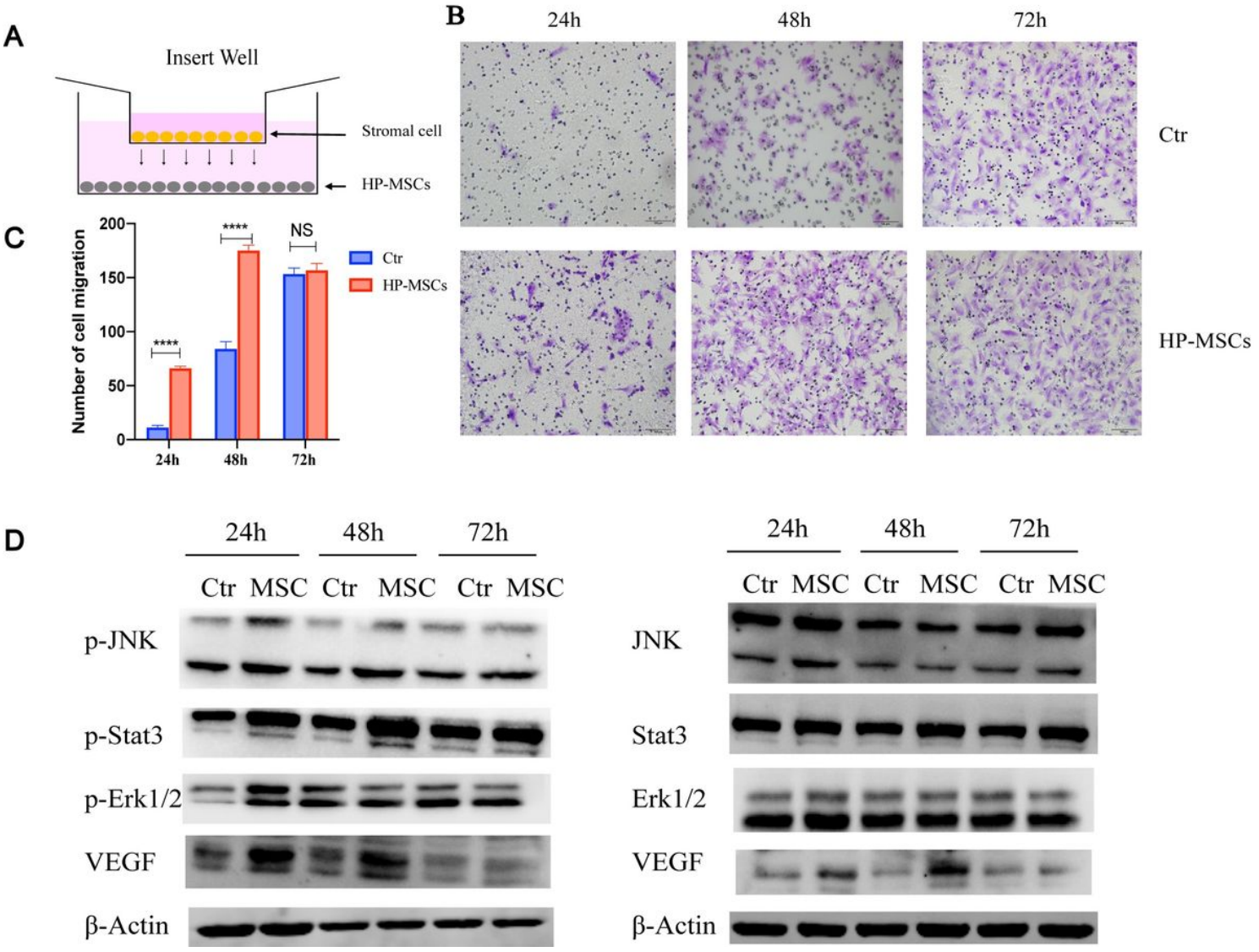

Figure 6

Effect of HP-MSCs on the migration of human endometrial stromal cells. (A) Schematic of co-culture of the stromal cells with HP-MSCs. Stromal cells were inoculated in the upper insert transwell (8 um), while HP-MSCs were in the lower hole plate. (B) Transwell migration assay was conducted at 24 h, 48 h, and 72 h, respectively, after culturing without and with HP-MSCs, respectively. The migrated cells were stained with purple. (C) The average number of migrated stromal cells after culturing without or with HP-MSCs for 24 h, 48 h, and 72 h, respectively (±SEM). *indicates P < 0.05, ** indicates P < 0.01, *** indicates P < 0.001. (D) p-JNK, p-Stat3, p-Erk1/2, VEGF, and corresponding total protein western blot analysis at 24 h, 48 h, and 72 h, respectively, after culturing without and with HP-MSCs, respectively.

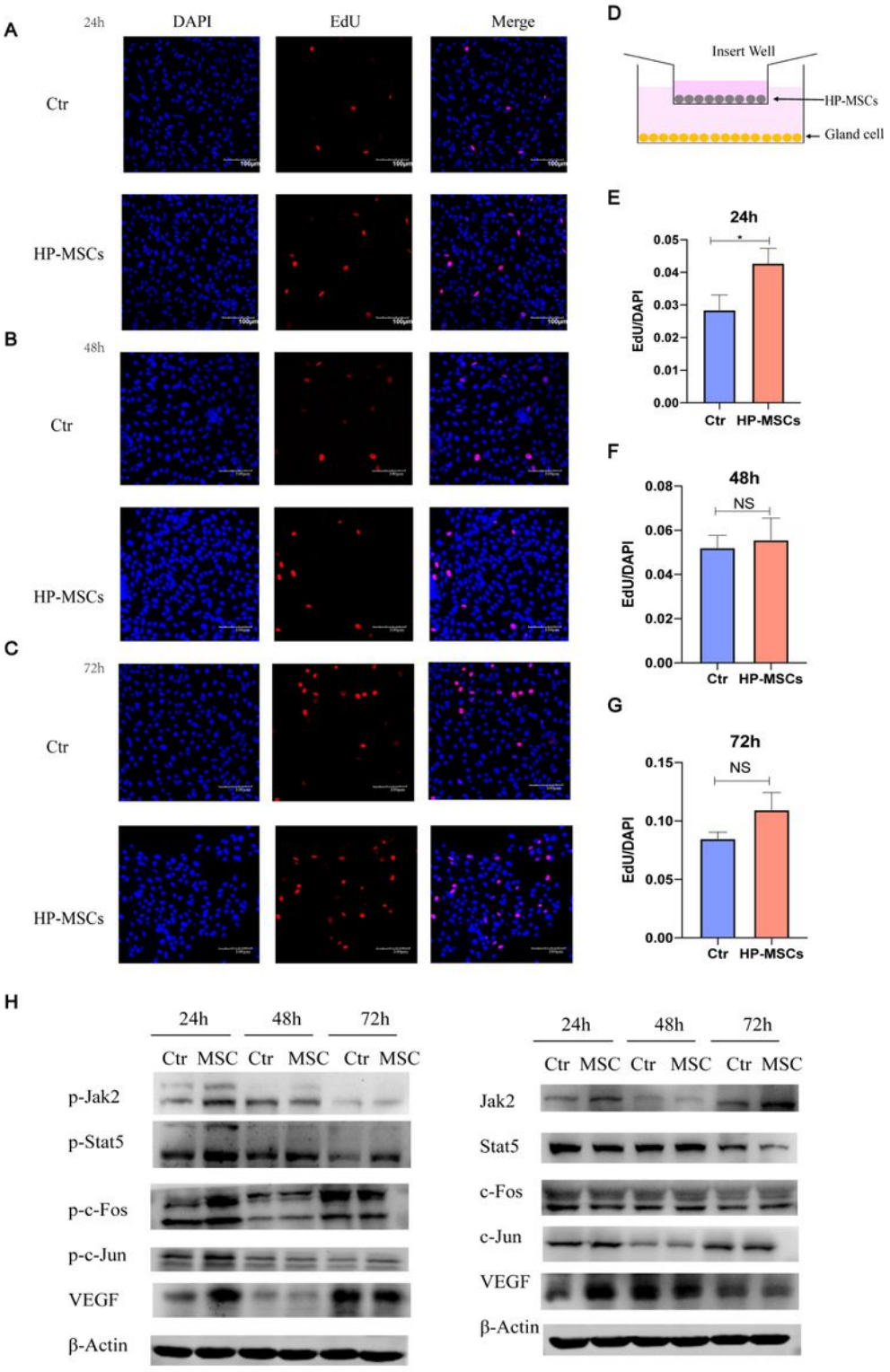

Figure 7

Effect of HP-MSCs on the proliferation of human endometrial glandular cells. (A-C) EdU assays were conducted after culturing of the glandular cells without and with HP-MSCs for 24 h, 48 h, 72 h, respectively. Representative confocal images of the glandular cells stained with EdU (red) and DAPI (blue). (D) Schematic of co-culture of the glandular cells with HP-MSCs. HP-MSCs were inoculated in the upper insert transwell (0.4um), while the glandular cells were in the bottom plate. (E-G) Average EdU/DAPI

ratio (±SEM). *indicates P < 0.05. (H) p-Jak2, p-Stat5, p-c-Fos, p-c-Jun, VEGF, and corresponding total protein western blot analysis at 24 h, 48 h, and 72 h, after culturing without and with HP-MSCs, respectively.

Supplementary Files

This is a list of supplementary files associated with this preprint. Click to download.

- SupplementalmaterialDanZhang.docx
- SupportingInformation.pdf
- GraphicalAbstract.jpg